



Barrier coatings with various types of cellulose nanofibrils and their barrier properties

Simyub Yook · Heetae Park · Hyeonji Park · Sun-Young Lee · Jaegyung Kwon · Hye Jung Youn 

Received: 30 November 2019 / Accepted: 12 February 2020 / Published online: 9 March 2020
© Springer Nature B.V. 2020

Abstract Needs for biodegradable packaging materials are growing to reduce the negative environmental impact of petroleum-based polymer packaging. Barrier paper packaging is in demand as environmentally-friendly barrier coating materials to improve biodegradability and recyclability. Cellulose nanofibril (CNF) is considered an alternative to conventional polymers for barrier coatings due to the barrier properties of its films. In this work, various types of CNFs were prepared and coated on linerboard and wood-free paper to evaluate the barrier properties of these papers against air, liquid water, water vapor, oxygen, and grease, and the major factors of the barrier

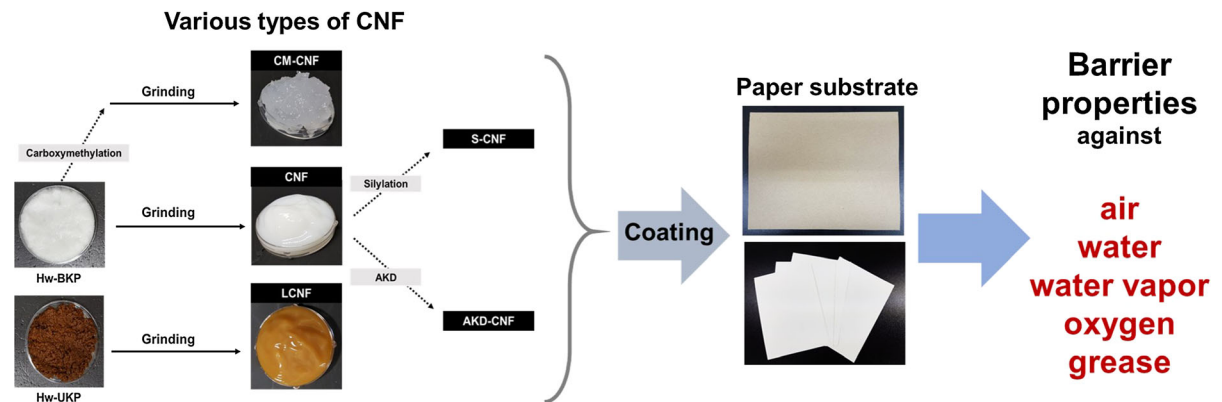
performance of the CNFs-based coatings were investigated. A coat weight of at least 10 g/m² was desirable to impart efficient the barrier properties to papers. The average fibril size and hydrophobicity were strongly related to the barrier properties. CNFs with smaller fibril sizes are beneficial for enhancing barrier properties, and hydrophobization improves the water resistance. Hydrophobic functional groups with sufficient chain lengths decreased the water vapor barrier properties. The average fibril diameter of CNFs may be related to the air resistance, oxygen barrier properties, and grease resistance.

S. Yook · H. Park · H. Park · H. J. Youn (✉)
Department of Forest Sciences, Seoul National
University, 1 Gwanak-ro, Gwanak-gu, Seoul 08826,
Republic of Korea
e-mail: page94@snu.ac.kr

S.-Y. Lee · J. Kwon
National Institute of Forest Sciences, 57 Heogiro,
Dongdaemun-gu, Seoul 02455, Republic of Korea

H. J. Youn
Research Institute of Agriculture and Life Sciences Seoul
National University, 1 Gwanak-ro, Gwanak-gu,
Seoul 08826, Republic of Korea

Graphic abstract



Keywords Barrier properties · Cellulose nanofibrils · Coating · Hydrophobization · Packaging paper

Introduction

Although paper is one of the most versatile materials for the packaging industry, paper cannot be used as a material for barrier packaging without special treatments, including extrusion or dispersion coating, and wax immersion. Barrier packaging materials need to resist permeation of substances such as water or gases from outside, which protects goods from deterioration. Most paper grades do not have sufficient barrier properties to preserve goods from decay and deterioration by preventing water or oxygen transmission because of the high porosity and hydrophilicity of papers. Hence, laminating polymers such as polyethylene (PE), polypropylene (PP), and ethylene vinyl alcohol (EVOH) are used to reduce the transmission of water vapor and oxygen gases in paper-based packaging, for example, food containers or cups (Riley 2012). That is, most barrier packaging papers contain plastic materials.

Plastics are a growing issue as an environmental hazard in recent years because most petroleum-based plastics are non-biodegradable (Leja and Lewandowicz 2010), non-renewable, and have low-recyclability. Discarded plastics have accumulated in the oceans (Efferth and Paul 2017), and microplastics threaten human health via the food chain (Smith et al. 2018). Therefore, the needs for biodegradable and renewable

materials are increasing in all industrial sectors including packaging materials.

Cellulose nanomaterials (CNMs), natural biodegradable polymers, can be applied as barrier materials in the form of films (Lavoine et al. 2012; Hubbe et al. 2017; Wang et al. 2018). Therefore, CNMs have been studied as an alternative for barrier packaging films because of their high barrier properties against oxygen. It is known that cellulose nanofibril (CNF) films are more beneficial than a cellulose nanocrystal (CNC) films for barrier properties because of the larger aspect ratio of CNFs (Belbekhouche et al. 2011). CNF coatings on paper have been studied as eco-friendly barrier packaging papers as well as CNF films. In previous studies, CNF coatings showed low permeability against air, grease, and oxygen, which can be advantageous as a barrier layer. It was reported that a higher coat weight of the CNF coating provides air resistance and grease resistance (Aulin et al. 2010; Kumar et al. 2016). The oxygen permeability of CNF film is one hundred times lower than that of polyethylene film (Lavoine et al. 2012; Wang et al. 2018). The oxygen transmission rate also decreases when the grammage of the CNF film increases (Aulin et al. 2010), and a microfibrillated cellulose (MFC) coating can decrease the oxygen transmission rate (Hult et al. 2010). However, a CNF coating cannot sufficiently decrease the water vapor transmission and wettability of paper. It was reported that a CNF coating provides water resistance, but CNF-coated papers are more absorptive than PE-laminated paper (Lavoine et al. 2014; Mousavi et al. 2018). As previous studies mentioned, water vapor barrier properties can be increased by

CNF coating, but the CNF coating has a limit to enhancing water vapor barrier properties. (Ferrer et al. 2017; Hubbe et al. 2017). Previous studies on CNF coatings as a barrier coating agent on paper have revealed the barrier and mechanical properties of CNF-coated papers; however, they did not investigate systematically the effects of various types of CNFs on the barrier properties. CNF properties can be varied by pretreatments, post-treatment, or selection of different types of raw materials.

Chemical pretreatment or lignin containing feedstock not only reduces the production cost of CNFs but also enhances the barrier properties of its films. Pretreatments, for example, carboxymethylation and TEMPO-oxidation, are conducted to reduce the nanofibrillation energy by inducing electrostatic repulsive forces between cellulose (Saito et al. 2006; Wågberg et al. 2008; Im et al. 2018). Carboxymethylated CNFs or TEMPO-oxidized CNFs can produce self-standing films or be coated on polymer films, which show higher barrier properties than CNF films from untreated pulps (Fukuzumi et al. 2009, 2013; Hubbe et al. 2017). Lignocellulosic nanofibrils (LCNFs), which are usually prepared from unbleached pulp, are applied to make barrier films. The presence of lignin suggests that lignocellulosic nanofibrils films can resist wetting (Rojo et al. 2015; Herrera et al. 2018).

CNF film or CNF-coated paper needs to overcome challenges such as water vapor barrier performance. Water molecules easily transmit through or are absorbed on hydrophilic cellulose films (Ferrer et al. 2017; Hubbe et al. 2017). To improve water vapor barrier property of CNF-based substances, incorporation of inorganic fillers or cross-linking agents and chemical modification of CNF have been introduced. Inorganic fillers or cross-linking could be added to enhance water vapor barrier performance of CNF films because these fillers give more tortuosity to CNF matrix (Spence et al. 2011; Tayeb and Tajvidi 2019). As water sorption behavior affects water vapor permeability of cellulose materials (Belbekhouche et al. 2011; Bedane et al. 2015), chemical modification for the hydrophobization of cellulose was also applied to prepare the barrier CNF films (Rodionova et al. 2011; Peresin et al. 2017; Solala et al. 2018). However, most hydrophobization processes require solvent exchange, which is an expensive, environmentally-unfriendly and time-consuming procedure. In recent

studies, hydrophobization in an aqueous system was proposed to solve the problems of solvent exchange. Silylation in an aqueous system was applied to prepare hydrophobic CNF aerogels, and the modified aerogels can absorb grease (Zhang et al. 2015; Zanini et al. 2017). AKD, which is a neutral sizing agent, can also modify CNF films with water repellent surfaces (Yang et al. 2014; Tarres et al. 2016; Goo et al. 2018).

In this study, we investigated the effects of the coat weight and the characteristics of the CNFs on the barrier properties of CNF-coated papers. Untreated CNFs produced from bleached kraft pulp were chosen as the control. Lignocellulosic nanofibrils were obtained from unbleached kraft pulp, and modified CNFs were prepared via carboxymethylation pretreatment and hydrophobization post-treatment. CNF and modified CNF coatings were conducted, and their barrier properties against air, liquid water, water vapor, oxygen, and grease were analyzed. We tried to clarify the major factors of the barrier coating using CNFs for accomplishing efficient barrier properties, and we aimed to suggest how to make an eco-friendly paper packaging material with high barrier performance.

Materials and methods

Materials

Never-dried hardwood bleached kraft pulp (Hw-BKP) and never-dried hardwood unbleached kraft pulp (Hw-UKP), which were supplied from Moorim P&P (Korea), were used for preparation of the CNF and LCNF. Monochloroacetic acid, isopropanol, hydrochloric acid, and sodium hydroxide were purchased as lab grade. Methyltrimethoxysilane (MTMS) was purchased from Sigma Aldrich, and an alkyl ketene dimer (AKD) emulsion was supplied by Taegwang Chemicals (Korea) for post-treatment with CNFs. Two different types of base paper, commercially produced linerboard (Taelim Paper, Korea) and wood-free base paper (Moorim Paper, Korea), were used for CNF coating. Table 1 shows the properties of the base papers.

Table 1 Properties of the base papers

	Linerboard	Wood-free base paper
Basis weight (g/m ²)	180 ± 1	215 ± 1
Apparent density (g/cm ³)	0.79	0.81
Gurley air permeability (s/100 cc)	40.4 ± 1.7	45.7 ± 2.6
Water contact angle (°)	21.5	67.9

Preparation and characterization of CNFs

To investigate how pretreatment or post-treatment of cellulose nanofibrils affects the barrier properties of the coated papers, five kinds of cellulose nanofibrils, untreated cellulose nanofibril (CNF), lignocellulose nanofibril (LCNF), carboxymethylated cellulose nanofibril (CM-CNF), silylated cellulose nanofibril (S-CNF) and AKD-added CNF (AKD-CNF), were prepared. CNF was prepared from Hw-BKP. A 2% Hw-BKP suspension was passed through a grinder (Masuko Sangyo, Japan) 20 times. The gap size was – 80 μm, and the rotor speed was 1,500 rpm. LCNF was prepared by grinding the Hw-UKP suspension in the same manner as the preparation of CNF. For the preparation of CM-CNF, Hw-BKP was first carboxymethylated according to the previously described method (Im et al. 2018). Carboxymethylated Hw-BKP was ground under the condition of CNF grinding, but the carboxymethylated pulp suspension was passed through the grinder 7 times. To improve the resistances against wetting and water vapor transmission, hydrophobization was performed as post-treatment using organosilane and AKD. S-CNF was prepared by adding hydrolyzed organosilane to a CNF suspension, which was adopted from Zhang's report (Zhang et al. 2015). MTMS was prehydrolyzed under acidic aqueous condition at pH 4, and then, prehydrolyzed MTMS was added to the CNF suspension at pH 4. The weight ratio of MTMS to CNF was 1:1. AKD-CNF was prepared by adding an AKD emulsion to a CNF suspension. The addition level of AKD was 3 to 5 wt% based on the oven dried weight of the CNFs. Figure 1 shows a scheme for preparing the different types of CNF suspensions for coating. The morphology of the CNFs was examined using field emission scanning electron microscopy (FE-SEM, Supra 55VP, Carl Zeiss, Germany), and the average width of the CNFs was determined by measuring the widths of a hundred fibrils in SEM images.

CNF coating on papers and characterization of the coating layer

CNF, LCNF, CM-CNF, S-CNF, and AKD-CNF suspensions were coated on the base papers using a laboratory coater (AB3120, TQC, Netherland) at a coating speed of 70 mm/s. The consistency of the CNF, LCNF, and AKD-CNF suspensions was adjusted to 1.5%. In the case of CM-CNF suspension, the consistency was adjusted to 1% to reduce the viscosity for even coating. The consistency of the S-CNF suspension was adjusted to 2%. Coat weights were controlled by a four-sided applicator with different gap sizes. Coated paper was dried in a hot air dryer at 120 °C and then passed through a drum dryer once. Coat weight was calculated by measuring the dried weights of the papers before and after coating. The morphology and hydrophobicity of the coating layer were investigated to examine the relationship between the barrier properties and the properties of coating layer. Surfaces and cross-sections of the coated papers were examined using FE-SEM. The hydrophobicity of five kinds of CNF-coated papers was evaluated by water contact angle (WCA) measurements. The water contact angle was measured in triplicate by DSA 100 (Krüss GmbH, Germany).

Evaluation of barrier properties

Barrier properties against air, water, water vapor, oxygen and grease were evaluated to investigate the effects of the CNF coating. Air resistance was measured by Gurley air permeability in accordance with TAPPI method T460. The amount of time required for 100 cc of air to permeate was measured. The upper limit of the instrument was 100,000 s/100 cc. Water resistance was evaluated by the Cobb test, which was performed in accordance with TAPPI method T441. A preconditioned specimen cut to 12.5 cm × 12.5 cm was fasten inside the Cobb tester. One hundred milliliters of deionized water was placed

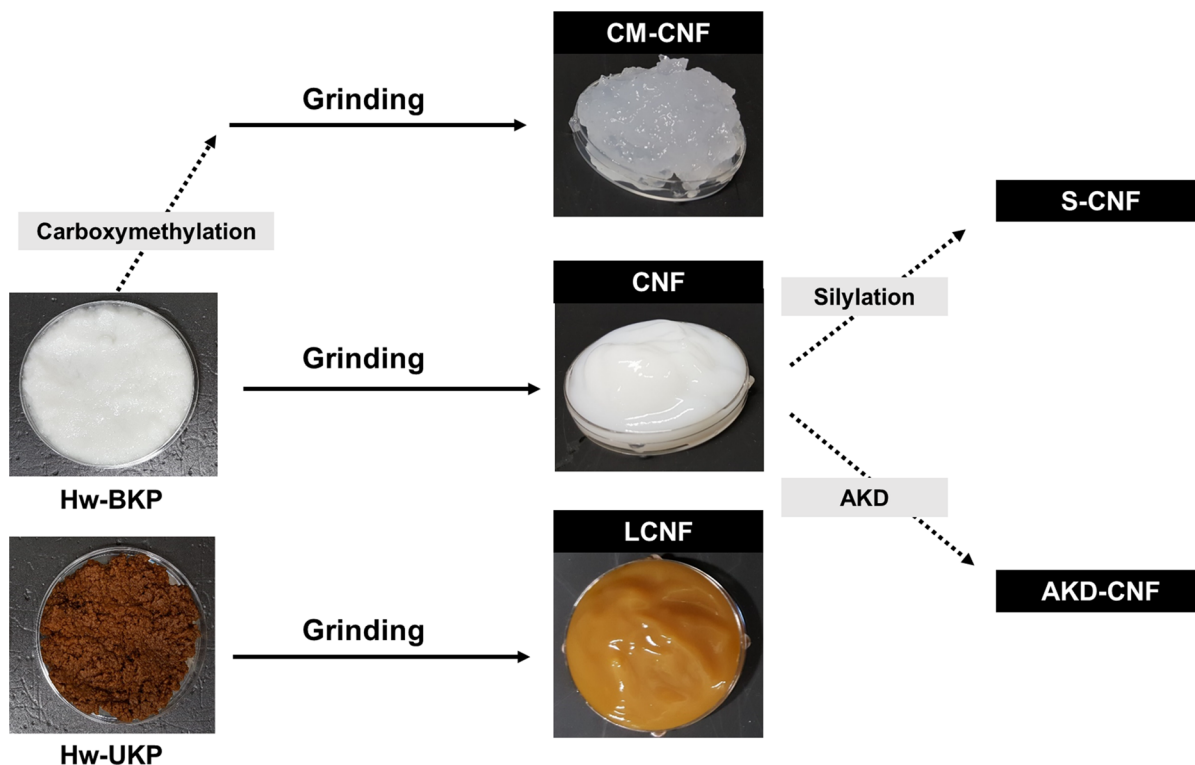


Fig. 1 A scheme for the preparation of different types of CNFs

inside the test ring. After 60 s of absorption, water was removed from the test equipment, and the remaining water was removed by blotting papers. The Cobb value was reported as the mass of absorbed water divided by the area of the circular ring. The water vapor transmission rate (WVTR) was evaluated in duplicate by TAPPI method T448. A specially designed cup containing oven-dried silica gel was sealed with the coated papers and sealants, and the assembled cup was then exposed for 24 h at 23 °C and 50% RH. The WVTR was calculated from the difference in weight before and after exposure for 24 h. The oxygen transmission rate (OTR) was determined with Illinois 8003 (Systech, USA) at 23° C and 0% RH, and the area of the measurement was at least 169 cm². Grease resistance was measured by a kit test in accordance with TAPPI method T 559. Kit solutions were made by mixing n-heptane, toluene, and castor oil, and then, the kit solutions were dropped on preconditioned specimens. If the solution darkened the coated paper, then a lower grade of kit solution was dropped until the solution did not stain the coated paper. The kit rating value was determined by the

grade of the kit solution that did not penetrate the coated paper, and the average kit number of five measurements was recorded.

Results and discussion

SEM observation of CNF-coated papers

Figure 2 shows the surface of the CNF-coated papers depending on the coat weight. Microscale pores were observed in uncoated paper, as shown in Fig. 2a. When the coat weight was 6 g/m², pores between pulp fibers were filled with CNFs, but the CNF coating was insufficient to cover the fibers completely because the appearance of fibers was noticeable on the surface. When the coat weight was approximately 10 g/m², the CNF coating layer covered the surface of the base papers completely, as shown in Fig. 2c. Figure 3 shows the cross-section images of the CNF-coated papers. Unlike the base paper, a CNF layer was formed on the surface of the papers in Fig. 3b, c, which is similar to those of the previous studies (Kumar et al.

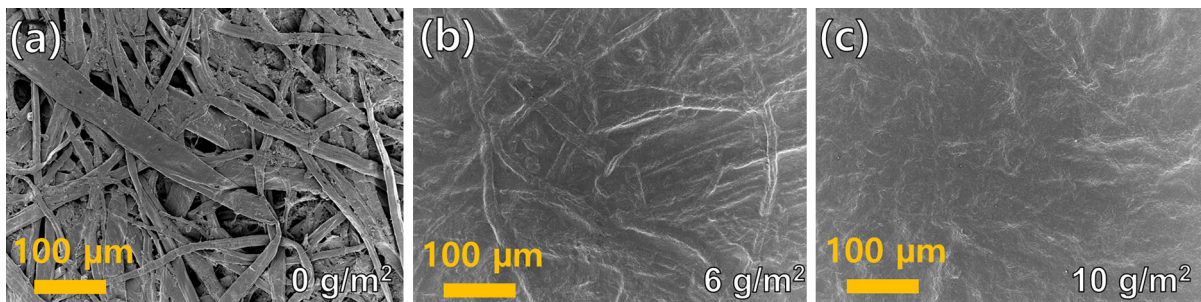


Fig. 2 Surface images of the CNF-coated wood-free paper with different coat weights (a: base paper, b: CNF at 6 g/m², c: CNF at 10 g/m²)

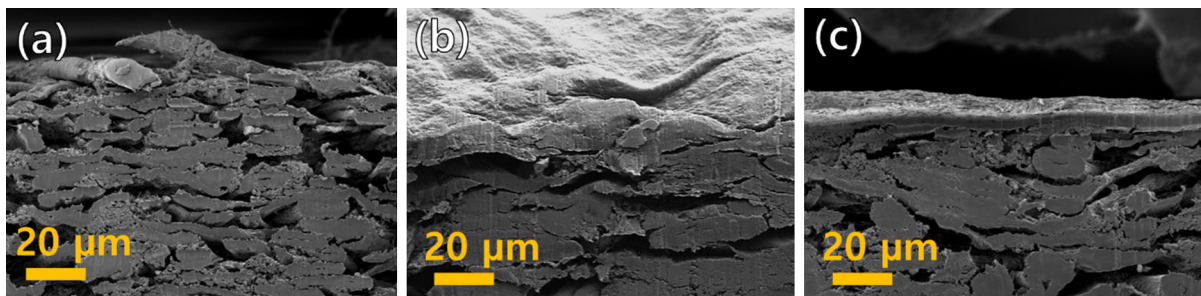


Fig. 3 Cross sectional images of the CNF-coated wood-free papers with different coat weights (a: base paper, b: CNF at 6 g/m², c: CNF at 10 g/m²)

2016, 2017; Mousavi et al. 2018). When the coat weight increased, the thickness of the coating layer increased. The CNF coating layer on the paper coated at high coat weight would be helpful for increasing barrier properties.

Figure 4 shows the surface images of the base paper, CNF-, LCNF-, CM-CNF-, S-CNF-, and AKD-CNF-coated papers with coat weights of approximately 10 g/m². CNFs formed a network by aggregation and entanglement, and the CNF layer totally covered the pores of the base papers. Compared to the CNF and LCNF coatings, the CM-CNF coating appeared to have denser coating layers with smaller pores. In the case of S-CNF and AKD-CNF, they were similar to CNF because silylation and AKD cannot change the structures of CNFs. The surface porosity of the coated papers was affected by the CNF morphology. Table 2 represents the average diameter of the various types of CNFs in this study. LCNF had the largest diameter among CNF types because lignin interfered with the nanofibrillation of unbleached pulps for the same number of grinding passes. The diameter of CM-CNF was the smallest due to the effect of carboxymethylation, which facilitates

nanofibrillation by imparting electrostatic repulsive forces between cellulose fibrils. In the case of S-CNF and AKD-CNF, their diameters were not significantly different from that of the untreated CNF, because post-treatments such as silylation or AKD addition did not affect the morphology. That is, chemical pretreatment of CNFs resulted in different morphologies and chemical properties of the untreated CNF, whereas post-treatment mainly affected the chemical properties of the CNFs. The difference in fibril morphology including diameter, length and aspect ratio may affect the structure of the CNF coating layer. A smaller CNF diameter can be advantageous for forming a denser coating layer, and CNFs with higher aspect ratio (smaller diameter and longer length) can improve barrier properties against air and oxygen because of increased tortuosity.

Air resistance

Figure 5a shows the Gurley air permeability of the CNF-coated wood-free paper with coat weight. Gurley air permeability exponentially increased with increasing coat weight for all types of CNF coatings. The

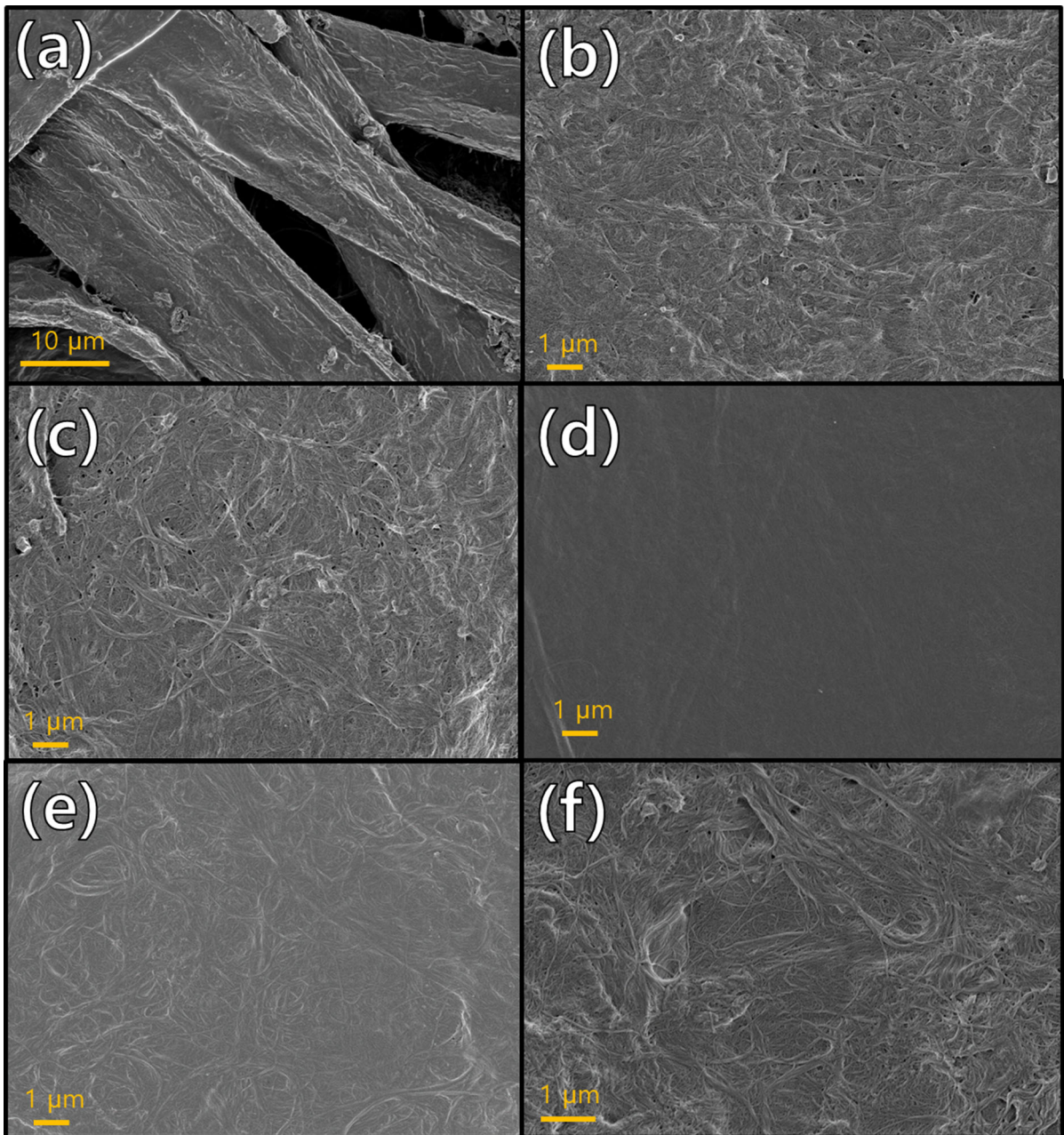


Fig. 4 SEM images of surface-coated wood-free paper with different types of CNFs at 10 g/m² (a: base paper, b: CNF, c: L-CNF, d: CM-CNF, e: S-CNF, f: AKD-CNF)

Table 2 Average diameter of the CNFs

Type	CNF	LCNF	CM-CNF	S-CNF	AKD-CNF
Average diameter (nm) (SD)	46 (17)	68 (20)	15 (3)	55 (11)	35 (18)

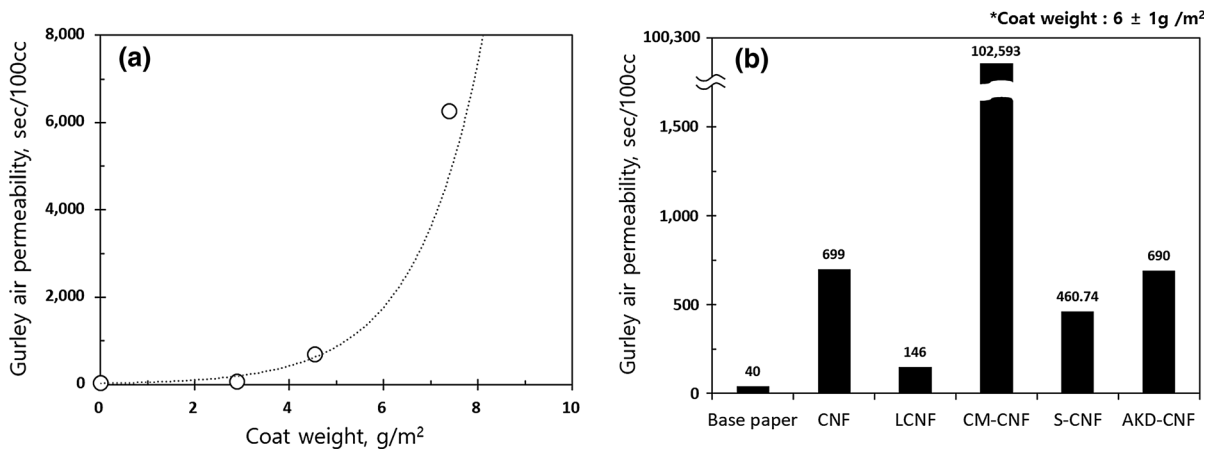


Fig. 5 Gurley air permeability of the coated linerboard papers depending on **a** coat weight and **b** various types of CNFs

Gurley air permeability of the base papers was approximately 40 s/100 cc, but it reached approximately 700 s/100 cc at the coat weight of 4.5 g/m² and exceeded the upper limit of the measurement at a coat weight of 10 g/m². Figure 5b shows the Gurley air permeability of the papers coated with different types of CNFs. Base paper, linerboard, had very low air permeation resistance, but the Gurley air permeability of the CNF-coated paper increased by 17 times that of the base paper, even at a coat weight of 6 g/m². The LCNF coating had lower Gurley air permeability than any other CNF coatings, whereas the CM-CNF coating exhibited the highest air permeation resistance, which was 147 times higher than that of the CNF coating. The S-CNF and AKD-CNF coatings had similar air permeation to the CNF coating. Several studies have reported that the coat weight significantly affects barrier properties because the coating layer is more uniform and thicker at high coat weights than at low coat weights (Aulin et al. 2010; Lavoine et al. 2014; Kumar et al. 2016). When comparing the results of LCNF- and CM-CNF-coated paper, fibrils with smaller diameters were helpful in preventing air permeation because they can form denser networks and decrease the pore size, which inhibits passage of substances such as air molecules (Spence et al. 2011). Post-treatments in this research did not affect the diameter of the CNFs significantly, so the S-CNF and AKD-CNF coatings resulted in Gurley permeability values similar to CNF.

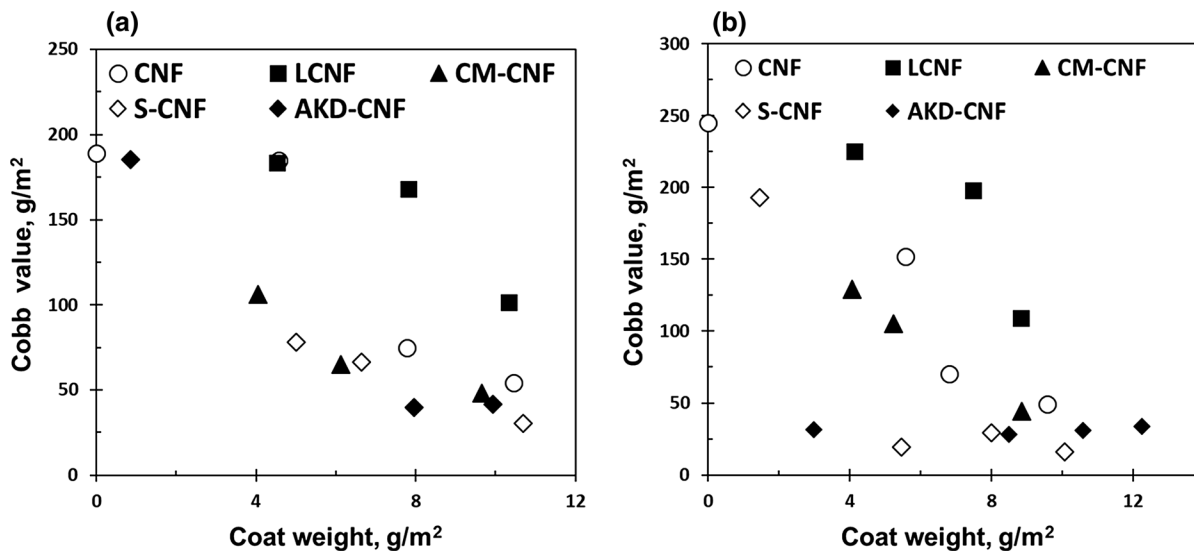
Water contact angle and Cobb value

Wettability is closely related to the surface chemical properties of a substance such as paper and CNF films (Washburn 1921). Table 3 shows the water contact angles of diverse types of CNF-coated papers at 1 s. Unlike the base paper, the WCA of the CNF-coated paper was approximately 40° due to the presence of the hydrophilic hydroxyl groups of cellulose. CM-CNF had a slightly higher WCA than CNF, but the CM-CNF coating was hydrophilic because carboxymethyl groups are ionic functional groups. The WCA of LCNF indicated that the coating layer was more hydrophobic than the CNF- and CM-CNF-coated papers due to the presence of lignin. However, the WCA of LCNF was smaller than 90° because of the hydrophilic groups that formed during the kraft pulping process (Ferrer et al. 2012). S-CNF and AKD-CNF had hydrophobic surfaces with WCAs over 90°. This means that silylation and AKD addition changed the surface chemical properties of CNFs from hydrophilic to hydrophobic by the introduction of hydrophobic functional groups to cellulose.

A high coat weight reduced the Cobb values of the coated papers, similar to the Gurley air permeability. Figure 6 shows the Cobb value of the coated linerboard and wood-free papers. When the coat weight increased, the Cobb value decreased rapidly. The reduction rate is dependent on the type of CNF. When the coat weight reached approximately 10 g/m², the Cobb value dropped by 75% in both the linerboard and wood-free paper, except for the LCNF coating. A high coat weight reduced the penetration of liquid water by

Table 3 Water contact angles of CNF coated papers

Type	Base paper	CNF	LCNF	CM-CNF	S-CNF	AKD-CNF
Average WCA at 1 s (°)	68	41	72	61	110	113

**Fig. 6** Cobb values of the coated papers with different types of CNFs (a: linerboard, b: wood-free paper)

eliminating pores and densely packed coating layers (Lavoine et al. 2014). In contrast, the low coat weight of CNF cannot ensure a barrier to water absorption though hydrophobized CNFs were applied on the paper. This was likely because the coverage or thickness of the CNF coating layer was not sufficient as shown Fig. 2.

The pre- or post-treatment of CNFs resulted in different Cobb value curves. The LCNF coating absorbed more water than any other CNF coating at similar coat weights, but S-CNF and AKD-CNF had lower Cobb values than the other CNF coatings at similar coat weights. The CM-CNF coating did not have a significant difference from the CNF coating in the case of the Cobb values. In short, hydrophobized S-CNF and AKD-CNF had better water resistances than CNF, and the LCNF coating had the highest wettability.

The effects of hydrophobization and fibril size caused the differences in the wettability of the coating layers. As shown in Table 3, hydrophobicity is one of the major factors determining the wettability of the coating layer. S-CNF and AKD-CNF were resistant to

water absorption when the coat weight was approximately 5 g/m². When CNFs were hydrophobized by silylation (Zhang et al. 2015; Zanini et al. 2017) or AKD addition (Yang et al. 2014; Goo et al. 2018), this interfered with water absorption. However, the wider diameter of LCNFs was adverse for preventing the absorption of liquid water, although the hydrophobicity of the LCNF was generally higher than that of the cellulose nanofibrils from the bleached pulp (Abe et al. 2009; Chinga-Carrasco et al. 2012; Herrera et al. 2018). This can be explained by the fact that the size of the voids also increases when the average width of the fibrils increases (Spence et al. 2011). Hence, liquid water can penetrate the coating layer due to the larger size of the pores. Despite the narrow diameter of CM-CNF, CM-CNF has a hydrophilic nature due to the presence of carboxymethyl groups attracting water molecules. Therefore, CM-CNF is not effective in preventing wetting and penetration unlike S-CNF or AKD-CNF.

WVTR

Chemical modification of CNFs affected the water vapor transmission rate of the coated papers at similar coat weights. Figure 7 depicts the WVTR values of the coated papers against the coat weight. The coat weight also affects the WVTR of the coated papers, such as the air permeability and water absorption. When the coat weight was approximately 10 g/m^2 , the differential of the WVTR curves was close to zero. The hydrophobization method of CNFs clearly affected water vapor transportation in the coating layer on both linerboard and wood-free base paper. The CNF, LCNF, and CM-CNF coatings had similar values, and the S-CNF-coated paper had a higher WVTR than the CNF-coated paper. AKD-CNF exhibited a low WVTR when the coat weight increased. The WVTR of the CNF-coated paper was approximately $300 \text{ g/m}^2 \cdot \text{day}$ which was about 55% reduction compared to base paper, whereas the AKD-CNF-coated paper exhibited approximately $100 \text{ g/m}^2 \cdot \text{day}$ at 10 g/m^2 coat weight. In summary, a coat weight of 10 g/m^2 decreased the WVTR, and AKD-CNF effectively decreased the WVTR among the examined CNFs in this study. It is difficult to compare our result with others in the literature because the type of base paper, CNF properties, and coating method are different. According to previous studies, CNF-coated papers have the WVTR ranging from 100 to $450 \text{ g/m}^2 \cdot \text{day}$. Mousavi et al. (2017) reported the gCNF-coated paper had

$390 \text{ g/m}^2 \cdot \text{day}$ at a coat weight of 4.4 g/m^2 . When carboxymethylcellulose (CMC) was added to CNF suspension, the coat weight increased but the WVTR of the gCNF/CMC-coated paper was not significantly improved. Kumar et al. (2016) reported the WVTR of approximately $100 \text{ g/m}^2 \cdot \text{day}$ by coating CNF/CMC suspension at 9 g/m^2 on linerboard using a roll-to-roll coater.

The effect of chemical modification can be explained by the mechanism of water vapor transportation via cellulose materials. Water vapor also passes through cellulose by successive sorption (Okubayashi et al. 2004), so the diffusion coefficient of CNF films is strongly related to the solubility of the surface (Belbekhouche et al. 2011). CNFs without chemical pretreatment have abundant hydroxyl groups, and CM-CNF had hydrophilic carboxyl groups with unreacted hydroxyl groups. Therefore, in the CNF and CM-CNF coatings, it was hard to reduce the solubility of water vapor even though CM-CNF formed denser films. Therefore, an increase in the coat weight can reduce the WVTR to a certain extent, but this is not a desirable solution to decrease water vapor sorption through a hydrophilic CNF coating layer. After all, a hydrophobic polymer or an inorganic filler can be a way to increase the water vapor barrier properties.

LCNF originated from lignin-rich unbleached pulps, and hydrophobic lignin may help interfere with

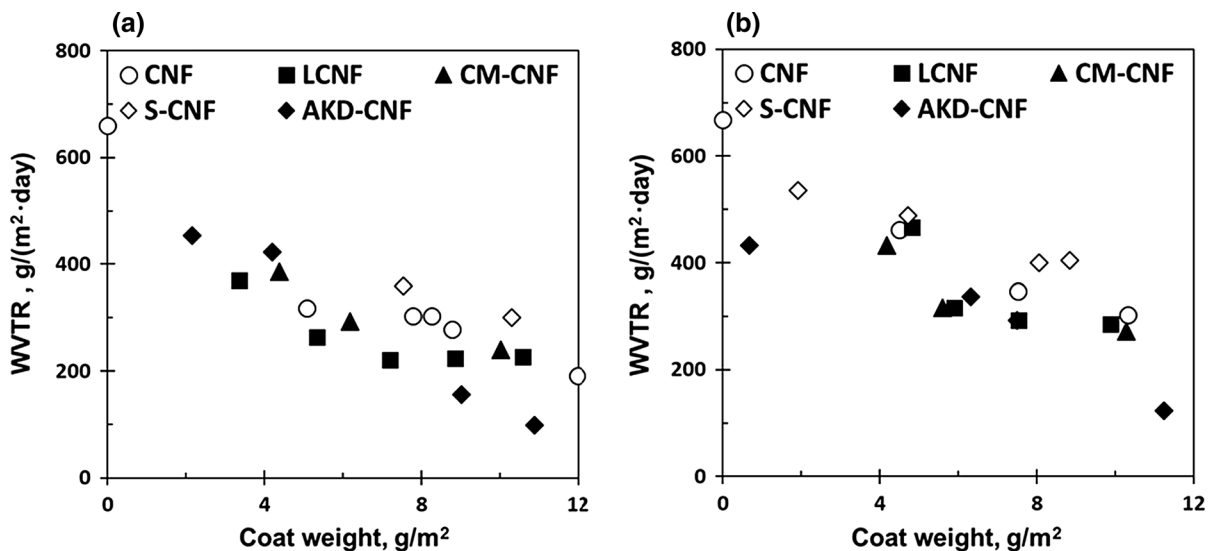


Fig. 7 Water vapor transmission rate of CNF coated papers with different types of CNFs (a: linerboard, b: wood-free paper)

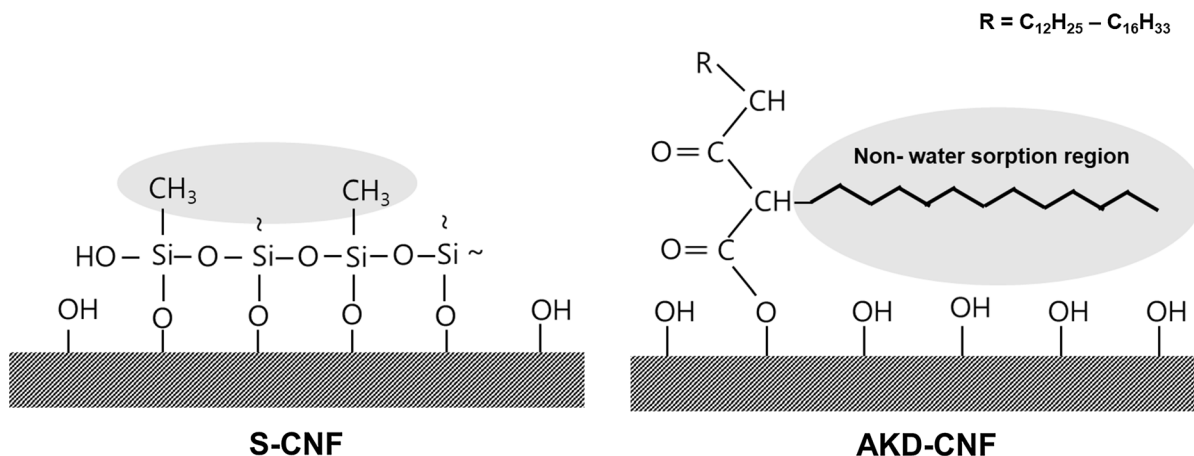


Fig. 8 A scheme of the chemical reaction of S-CNF- and AKD-CNF-coated papers

the sorption of water vapor on the LCNF coating. Despite the presence of lignin, the LCNF coating had a similar WVTR to CNF because the hydrophobicity of lignin was not enough to decrease the sorption of water vapor. Both S-CNF and AKD-CNF were hydrophobized CNFs, which was confirmed by their WCA values. However, the WVTR values of the S-CNF- and AKD-CNF-coated papers were surprisingly different. The chemical structure of MTMS and AKD may induce differences in water vapor sorption. MTMS was hydrolyzed in water, and bonded with other MTMS or hydroxyl groups of cellulose (Zhang et al. 2015). Therefore, S-CNF had silanol groups and short alkyl groups from MTMS. Otherwise, AKD had long alkyl groups and bound with CNFs by β -keto ester bonds. As shown in Fig. 8, hydrophobic groups in S-CNF might not prevent effective transportation of water vapor because of the short length of the hydrophobic alkyl groups. Hydrophobic chains from AKD may effectively interrupt the sorption of water vapors. In short, a long chain length is advantageous for the prevention of water vapor transmission.

OTR

Oxygen transmission also decreased with the coat weight and modification of CNFs. Figure 9 shows the OTR values of the coated papers, and the upper limit of the OTR measurement instrument was $400,000 \text{ cm}^3/\text{m}^2\cdot\text{day}$. A coat weight under a certain value did not show detectable oxygen barrier properties. For instance, the OTR of the CNF coating at 5 g/m^2 was at

the upper limit, which indicates no barrier to oxygen. Modification of CNFs may also affect the OTR values at a high coat weight. CM-CNF had a lower OTR value than the CNF coating. In contrast, the LCNF coating was permeable against oxygen regardless of the coat weight. Only the LCNF coating on linerboard at 10 g/m^2 reduced the OTR values. S-CNF and AKD-CNF also did not have barrier properties at coat weights lower than 9 g/m^2 , and the reduction rate of S-CNF was smaller than that of CNF. In the case of AKD-CNF coating, the coated papers had a lower oxygen transmission rate than the CNF coating.

These results revealed that the morphological and chemical characteristics of CNFs might affect the oxygen barrier properties. In the literature, CNF films or CNF coatings on polylactic acid films showed low OTR and oxygen permeability, for example, $0.5\text{--}1.0 \text{ cc}\cdot\mu\text{m}^2\cdot\text{day}\cdot\text{kPa}$ (Ferrer et al. 2017; Roilo et al. 2017), because of the dense packing structure of the CNF film (Aulin et al. 2010; Lavoine et al. 2012; Hubbe et al. 2017). Smaller diameter fibrils can reduce the average size of pores and increase the contour length of the pathway, according to the literature (Ottesen et al. 2017). This clue is one of the reasons why fibrils with smaller diameters are more advantageous for decreasing the OTR. In the case of S-CNF and AKD-CNF, the fibril diameter did not affect the diffusion of oxygen. Nonpolar gases, such as oxygen, are difficult to solubilize on cellulose (Belbekhouche et al. 2011), so low diffusivity is the main barrier mechanism of oxygen transmission in cellulose nanofibrils films (Fukuzumi et al. 2013). In the case

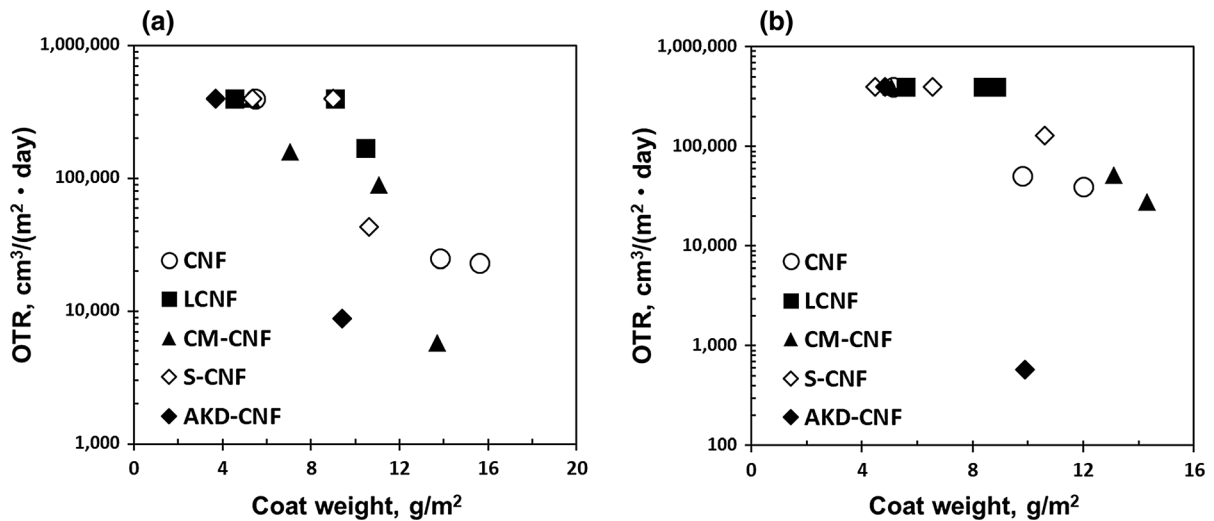


Fig. 9 Oxygen transmission rate of the coated papers (**a**: linerboard, **b**: wood-free paper)

of untreated CNF, it is proposed that interactions between fibrils contribute to the interference with the diffusion of oxygen (Hubbe et al. 2017). If CNFs are functionalized toward nonpolar surfaces via hydrophobization, oxygen can be transmitted via substituted functional groups (Peresin et al. 2017). MTMS was added as 100% of the oven dried weight of CNFs in S-CNF, so substituted areas would be a pathway for oxygen transmission. Otherwise, when AKD was added as 3% of the oven dried weight of the CNFs in AKD-CNF, hydroxyl groups may remain unreacted. Unreacted hydroxyl groups may be available to form networks that interfere with oxygen transmission. Hence, the fibril width and chemical properties affect the oxygen permeability of the CNF coating layer. However, the OTR values were too high for use as barrier packaging paper, and should be improved by developing an effective coating structure or incorporating other coating materials.

Grease resistance

The grease resistance of the coated papers evaluated by the kit test method is plotted in Fig. 10. In the kit test method, when the kit number is close to 12, the grease resistance of the specimen is high. The 0 kit number means that a specimen does not have grease resistance. The graph shows that a higher coat weight of CNF enhanced the grease resistance of the coated papers, similar to other barrier properties. For

example, a 4 g/m² CNF coating showed kit number of 1.5, whereas 9 g/m² CNF coating exhibited a more impenetrable surface, with a 12 kit number. LCNF more rapidly absorbed grease than CNF at a similar coat weight, so the kit number of LCNF was lower than other CNFs. Conversely, CM-CNF had higher kit values than CNF. For example, the CM-CNF coating was 9.7 kit number, while the CNF coating was 1.5 kit number. S-CNF and AKD-CNF had a similar tendency to CNF, but the hydrophobized CNFs had a lower kit number than the CNF coating.

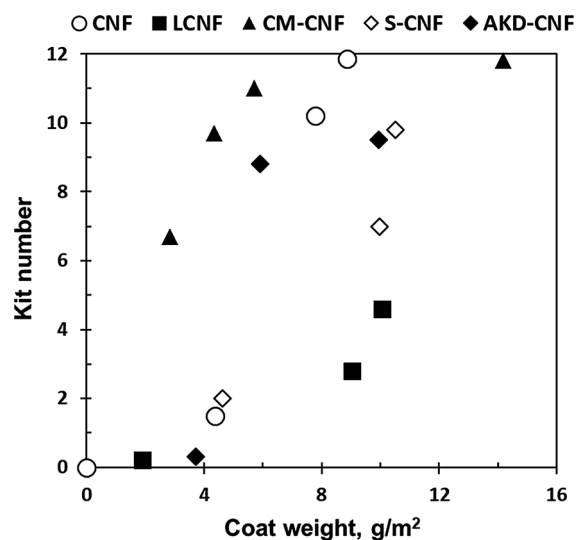


Fig. 10 Grease resistance (kit number) of the coated wood-free papers

The greater grease resistance of the coated papers depended on the diameter of the CNFs, such as the Gurley air permeability, which could be found in the literature. According to Mousavi et al. (2018), gCNF-coated paperboard showed approximately 9 kit number at a coat weight of 9 g/m², and rCNF exhibited lower kit value than 2 at 8 g/m² coat weight. The most fibrils of gCNF have a diameter between 20 and 40 nm, whereas most of rCNF fibrils are larger than 100 nm. It also indicates that the diameter of CNFs affects grease resistance. The grease resistance of CNF-coated papers showed a relationship with the air resistance of the coated papers, as mentioned previously (Aulin et al. 2010; Kumar et al. 2016; Mousavi et al. 2017). In the literature, smaller pores interrupted the penetration of grease and air by extending the path (Aulin et al. 2010). Hence, CM-CNF had a higher resistance than other CNF coatings. However, CNF coatings with small diameters are needed to obtain a high grease resistance. Hydrophobization of CNFs means that some hydroxyl groups are substituted by hydrophobic chains, such as aliphatic carbon chain. The intrinsic hydrophilicity and hydrogen bonds of CNFs have been suggested to provide the grease barrier properties of CNF coatings in previous studies (Aulin et al. 2012; Kumar et al. 2014; Hubbe et al. 2017). The presence of siloxane and long alkyl groups may cause a loosening effect in the hydrogen bonds between CNFs. Therefore, the S-CNF coating and AKD-CNF coating exhibited a lightly lower grease resistance than the CNF coating.

Conclusions

Various types of CNFs were investigated as barrier coating materials to produce eco-friendly packaging with improved barrier properties. Five different types of cellulose nanofibrils, CNF, LCNF, CM-CNF, S-CNF, and AKD-CNF, were prepared by grinding BKP and UKP and pre- and post-treatment steps. The materials were coated on linerboard and wood-free papers with different coat weights. The barrier properties against air, liquid water, water vapor, oxygen, and grease were examined depending on the coat weight and CNF type. The coat weight of the CNFs had a strong impact on the barrier performance, and the coat weight for effective barrier properties was 10 g/m². The LCNF-coated paper was the most

permeable in this study. The CM-CNF coating exhibited better barrier properties than the CNF coating. Both organosilane and AKD made hydrophobic coating layers, so the S-CNF- and AKD-CNF-coatings increased the water resistance. However, only the AKD-CNF coating enhanced the water vapor barrier properties due to the presence of long alkyl chains. Based on these results, it was found that the coat weight must reach a certain level to show barrier properties. A low coat weight cannot provide barrier properties due to insufficient coverage and thickness. In this study, 10 g/m² is a suitable coat weight for noticeable barrier performance against air, liquid water, water vapor, and grease. Second, a smaller CNF diameter is advantageous for reducing the permeation of substances such as water vapor and oxygen. Finally, hydrophobization of CNFs is beneficial to enhance water-related barrier properties, and the functional group of the hydrophobic chemical affects water vapor transmission. Modified CNF coatings decreased wettability, but the difference in functional groups induced a discrepancy in the barrier properties against water vapor and oxygen. Air resistance, oxygen barrier properties and grease resistance were mainly related to the average fibril diameter, and the fibril diameter should be narrow at a certain value. Further study on a strategy for CNF coating to remarkably improve barrier properties against water vapor and oxygen is needed.

Acknowledgments This work was fully funded by National Institute of Forest Sciences (FP0400-2016-01).

References

- Abe K, Nakatsubo F, Yano H (2009) High-strength nanocomposite based on fibrillated chemi-thermomechanical pulp. *Compos Sci Technol* 69:2434–2437. <https://doi.org/10.1016/j.compscitech.2009.06.015>
- Aulin C, Gällstedt M, Lindström T (2010) Oxygen and oil barrier properties of microfibrillated cellulose films and coatings. *Cellulose* 17:559–574. <https://doi.org/10.1007/s10570-009-9393-y>
- Aulin C, Salazar-Alvarez G, Lindström T (2012) High strength, flexible and transparent nanofibrillated cellulose–nanoclay biohybrid films with tunable oxygen and water vapor permeability. *Nanoscale* 4:6622–6628. <https://doi.org/10.1039/C2NR31726E>
- Bedane AH, Eić M, Farmahini-Farahani M, Xiao H (2015) Water vapor transport properties of regenerated cellulose

- and nanofibrillated cellulose films. *J Membr Sci* 493:46–57. <https://doi.org/10.1016/j.memsci.2015.06.009>
- Belbekhouche S, Bras J, Siqueira G, Chappey C, Lebrun L, Khelifi B, Marais S, Dufresne A (2011) Water sorption behavior and gas barrier properties of cellulose whiskers and microfibrils films. *Carbohydr Polym* 83:1740–1748. <https://doi.org/10.1016/j.carbpol.2010.10.036>
- Chinga-Carrasco G, Kuznetsova N, Garaeva M, Leirset I, Gallullina G, Kostochko A, Syverud K (2012) Bleached and unbleached MFC nanobarriers: properties and hydrophobisation with hexamethyldisilazane. *J Nanopart Res* 14:1280. <https://doi.org/10.1007/s11051-012-1280-z>
- Effertth T, Paul NW (2017) Threats to human health by great ocean garbage patches. *Lancet Planet Health* 1:e301–e303. [https://doi.org/10.1016/S2542-5196\(17\)30140-7](https://doi.org/10.1016/S2542-5196(17)30140-7)
- Ferrer A, Quintana E, Filpponen I, Solala I, Vidal T, Rodríguez A, Laine J, Rojas OJ (2012) Effect of residual lignin and heteropolysaccharides in nanofibrillar cellulose and nanopaper from wood fibers. *Cellulose* 19:2179–2193. <https://doi.org/10.1007/s10570-012-9788-z>
- Ferrer A, Pal L, Hubbe M (2017) Nanocellulose in packaging: advances in barrier layer technologies. *Ind Crops Prod* 95:574–582. <https://doi.org/10.1016/j.indcrop.2016.11.012>
- Fukuzumi H, Saito T, Iwata T, Kumamoto Y, Isogai A (2009) Transparent and high gas barrier films of cellulose nanofibers prepared by TEMPO-mediated oxidation. *Biomacromol* 10:162–165. <https://doi.org/10.1021/bm801065u>
- Fukuzumi H, Fujisawa S, Saito T, Isogai A (2013) Selective permeation of hydrogen gas using cellulose nanofibril film. *Biomacromol* 14:1705–1709. <https://doi.org/10.1021/bm400377e>
- Goo S, Park H, Yook S, Park SY, Youn HJ (2018) Preparation of hydrophobized cellulose nanofibril film with high strength using AKD. *J Korea TAPPI* 50(6):34–41. <https://doi.org/10.7584/JKTAPPI.2018.12.50.6.34>
- Herrera M, Thitiwutthisakul K, Yang X, Rujitanaroj P-o, Rojas R, Berglund L (2018) Preparation and evaluation of high-lignin content cellulose nanofibrils from eucalyptus pulp. *Cellulose* 25:3121–3133. <https://doi.org/10.1007/s10570-018-1764-9>
- Hubbe MA, Ferrer A, Tyagi P, Yin Y, Salas C, Pal L, Rojas OJ (2017) Nanocellulose in thin films, coatings, and plies for packaging applications: a review. *BioResources* 12(1):2143–2233
- Hult E-L, Iotti M, Lenés M (2010) Efficient approach to high barrier packaging using microfibrillar cellulose and shellac. *Cellulose* 17:575–586. <https://doi.org/10.1007/s10570-010-9408-8>
- Im W, Lee S, Rajabi Abhari A, Youn HJ, Lee HL (2018) Optimization of carboxymethylation reaction as a pre-treatment for production of cellulose nanofibrils. *Cellulose* 25:3873–3883. <https://doi.org/10.1007/s10570-018-1853-9>
- Kumar V, Bollström R, Yang A, Chen Q, Chen G, Salminen P, Bousfield D, Toivakka M (2014) Comparison of nano- and microfibrillated cellulose films. *Cellulose* 21:3443–3456. <https://doi.org/10.1007/s10570-014-0357-5>
- Kumar V, Elfving A, Koivula H, Bousfield D, Toivakka M (2016) Roll-to-roll processed cellulose nanofiber coatings. *Ind Eng Chem Res* 55:3603–3613. <https://doi.org/10.1021/acs.iecr.6b00417>
- Kumar V, Koppolu VR, Bousfield D, Toivakka M (2017) Substrate role in coating of microfibrillated cellulose suspensions. *Cellulose* 24:1247–1260. <https://doi.org/10.1007/s10570-017-1201-5>
- Lavoine N, Desloges I, Dufresne A, Bras J (2012) Microfibrillated cellulose—its barrier properties and applications in cellulosic materials: a review. *Carbohydr Polym* 90:735–764. <https://doi.org/10.1016/j.carbpol.2012.05.026>
- Lavoine N, Bras J, Desloges I (2014) Mechanical and barrier properties of cardboard and 3D packaging coated with microfibrillated cellulose. *J Appl Polym Sci* 131:1–11. <https://doi.org/10.1002/app.40106>
- Leja K, Lewandowicz G (2010) Polymer biodegradation and biodegradable polymers—a review. *Pol J Environ Stud* 19:255–266
- Mousavi SMM, Afra E, Tajvidi M, Bousfield DW, Dehghani-Firouzabadi M (2017) Cellulose nanofiber/carboxymethyl cellulose blends as an efficient coating to improve the structure and barrier properties of paperboard. *Cellulose* 24:3001–3014. <https://doi.org/10.1007/s10570-017-1299-5>
- Mousavi SMM, Afra E, Tajvidi M, Bousfield DW, Dehghani-Firouzabadi M (2018) Application of cellulose nanofibril (CNF) as coating on paperboard at moderate solids content and high coating speed using blade coater. *Prog Org Coat* 122:207–218. <https://doi.org/10.1016/j.porgcoat.2018.05.024>
- Okubayashi S, Griesser UJ, Bechtold T (2004) A kinetic study of moisture sorption and desorption on lyocell fibers. *Carbohydr Polym* 58:293–299. <https://doi.org/10.1016/j.carbpol.2004.07.004>
- Ottesen V, Kumar V, Toivakka M, Carrasco Gary C, Syverud K, Gregersen Øyvind W (2017) Viability and properties of roll-to-roll coating of cellulose nanofibrils on recycled paperboard. *Nord Pulp Pap Res J* 32:179. <https://doi.org/10.3183/npprj-2017-32-02-p179-188>
- Peresin MS, Kammiovirta K, Heikkinen H, Johansson L-S, Vartiainen J, Setälä H, Österberg M, Tammelin T (2017) Understanding the mechanisms of oxygen diffusion through surface functionalized nanocellulose films. *Carbohydr Polym* 174:309–317. <https://doi.org/10.1016/j.carbpol.2017.06.066>
- Riley A (2012) Paper and paperboard packaging. In: Emblem A, Emblem H (eds) *Packaging technology: fundamentals, materials and processes*, 1st edn. Woodhead Publishing, Cambridge.
- Rodionova G, Lenés M, Eriksen Ø, Gregersen Ø (2011) Surface chemical modification of microfibrillated cellulose: improvement of barrier properties for packaging applications. *Cellulose* 18:127–134. <https://doi.org/10.1007/s10570-010-9474-y>
- Roilo D, Maestri CA, Scarpa M, Bettotti P, Egger W, Koschine T, Brusa RS, Checchetto R (2017) Cellulose nanofibrils films: molecular diffusion through elongated sub-nano cavities. *J Phys Chem C* 121(28):15437–15447. <https://doi.org/10.1021/acs.jpcc.7b02895>
- Rojo E, Peresin MS, Sampson WW, Hoeger IC, Vartiainen J, Laine J, Rojas OJ (2015) Comprehensive elucidation of the

- effect of residual lignin on the physical, barrier, mechanical and surface properties of nanocellulose films. *Green Chem* 17:1853–1866. <https://doi.org/10.1039/c4gc02398f>
- Saito T, Nishiyama Y, Putaux JL, Vignon M, Isogai A (2006) Homogeneous suspensions of individualized microfibrils from TEMPO-catalyzed oxidation of native cellulose. *Biomacromol* 7:1687–1691. <https://doi.org/10.1021/bm060154s>
- Smith M, Love DC, Rochman CM, Neff RA (2018) Microplastics in seafood and the implications for human health. *Curr Environ Health Rep* 5:375–386. <https://doi.org/10.1007/s40572-018-0206-z>
- Solala I, Bordes R, Larsson A (2018) Water vapor mass transport across nanofibrillated cellulose films: effect of surface hydrophobization. *Cellulose* 25:347–356. <https://doi.org/10.1007/s10570-017-1608-z>
- Spence KL, Venditti RA, Rojas OJ, Pawlak JJ, Hubbe MA (2011) Water vapor barrier properties of coated and filled microfibrillated cellulose composite films. *BioResources* 6:4370–4888
- Tarres Q, Oliver-Ortega H, Llop M, Pelach MA, Delgado-Aguilar M, Mutje P (2016) Effective and simple methodology to produce nanocellulose-based aerogels for selective oil removal. *Cellulose* 23:3077–3088. <https://doi.org/10.1007/s10570-016-1017-8>
- Tayeb AH, Tajvidi M (2019) Sustainable barrier system via self-assembly of colloidal montmorillonite and cross-linking resins on nanocellulose interfaces. *ACS Appl Mater Interfaces* 11:1604–1605. <https://doi.org/10.1021/acsami.8b16659>
- Wågberg L, Decher G, Norgren M, Lindstrom T, Ankerfors M, Axnas K (2008) The build-up of polyelectrolyte multilayers of microfibrillated cellulose and cationic polyelectrolytes. *Langmuir* 24:784–795. <https://doi.org/10.1021/la702481v>
- Wang J, Gardner DJ, Stark NM, Bousfield DW, Tajvidi M, Cai Z (2018) Moisture and oxygen barrier properties of cellulose nanomaterial-based films. *ACS Sustain Chem Eng* 6(1):49–70. <https://doi.org/10.1021/acssuschemeng.7b03523>
- Washburn EW (1921) The dynamics of capillary flow. *Phys Rev* 17:273–283. <https://doi.org/10.1103/PhysRev.17.273>
- Yang Q, Takeuchi M, Saito T, Isogai A (2014) Formation of nanosized islands of dialkyl beta-ketoester bonds for efficient hydrophobization of a cellulose film surface. *Langmuir* 30:8109–8118. <https://doi.org/10.1021/la501706t>
- Zanini M, Lavoratti A, Lazzari LK, Galiotto D, Pagnocelli M, Baldasso C, Zattera AJ (2017) Producing aerogels from silanized cellulose nanofiber suspension. *Cellulose* 24:769–779. <https://doi.org/10.1007/s10570-016-1142-4>
- Zhang Z, Tingaut P, Rentsch D, Zimmermann T, Sebe G (2015) Controlled silylation of nanofibrillated cellulose in water: reinforcement of a model polydimethylsiloxane network. *Chemsuschem* 8:2681–2690. <https://doi.org/10.1002/cssc.201500525>

Publisher's Note Springer Nature remains neutral with regard to jurisdictional claims in published maps and institutional affiliations.